



Molecular Crystals and Liquid Crystals Incorporating Nonlinear Optics

Publication details, including instructions for authors and
subscription information:

<http://www.tandfonline.com/loi/gmcl17>

Structural and Electronic Properties of TXF-TCNQ (X = S, Se, Te)

Dwaine O. Cowan^a, Michael D. Mays^a, Thomas J. Kistenmacher^b,
Theodore O. Poehler^b, Mark A. Beno^c, Aravinda M. Kini^c, Jack M.
Williams^c, Yai-Kwong Kwok^c, K. Douglas Carlson^c, Li Xiao^d, Juan
J. Novoa^d & Myung-Hwan Whangbo^d

^a Department of Chemistry, The Johns Hopkins University, Baltimore,
Maryland, 21218

^b Applied Physics Laboratory, The Johns Hopkins University, Laurel,
Maryland, 20707

^c Chemistry and Materials Science Divisions, Argonne National
Laboratory, Argonne, Illinois, 60439

^d Department of Chemistry, North Carolina State University, Raleigh,
North Carolina, 27695-8204

Version of record first published: 22 Sep 2006.

To cite this article: Dwaine O. Cowan, Michael D. Mays, Thomas J. Kistenmacher, Theodore O. Poehler, Mark A. Beno, Aravinda M. Kini, Jack M. Williams, Yai-Kwong Kwok, K. Douglas Carlson, Li Xiao, Juan J. Novoa & Myung-Hwan Whangbo (1990): Structural and Electronic Properties of TXF-TCNQ (X = S, Se, Te), *Molecular Crystals and Liquid Crystals Incorporating Nonlinear Optics*, 181:1, 43-58

To link to this article: <http://dx.doi.org/10.1080/00268949008035991>

PLEASE SCROLL DOWN FOR ARTICLE

Full terms and conditions of use: <http://www.tandfonline.com/page/terms-and-conditions>

This article may be used for research, teaching, and private study purposes. Any substantial or systematic reproduction, redistribution, reselling, loan, sub-licensing, systematic supply, or distribution in any form to anyone is expressly forbidden.

The publisher does not give any warranty express or implied or make any representation that the contents will be complete or accurate or up to date. The accuracy of any instructions, formulae, and drug doses should be independently verified with primary sources. The publisher shall not be liable for any loss, actions, claims, proceedings,

demand, or costs or damages whatsoever or howsoever caused arising directly or indirectly in connection with or arising out of the use of this material.

STRUCTURAL AND ELECTRONIC PROPERTIES OF TXF - TCNQ (X = S, Se, Te)

DWAINE O. COWAN AND MICHAEL D. MAYS
Department of Chemistry, The Johns Hopkins University, Baltimore,
Maryland 21218

THOMAS J. KISTENMACHER AND THEODORE O. POEHLER
Applied Physics Laboratory, The Johns Hopkins University, Laurel,
Maryland 20707

MARK A. BENO, ARAVINDA M. KINI, JACK M. WILLIAMS, YAI-
KWONG KWOK AND K. DOUGLAS CARLSON
Chemistry and Materials Science Divisions, Argonne National Laboratory,
Argonne, Illinois 60439

LI XIAO, JUAN J. NOVOA AND MYUNG-HWAN WHANGBO
Department of Chemistry, North Carolina State University, Raleigh,
North Carolina 27695-8204

Abstract We report the crystal structure and physical properties of TTeF-TCNQ, compare the electrical conductivities of TXF-TCNQ (X = S, Se, Te) by performing tight-binding band calculations on TXF-TCNQ, and examine the differences in the packing patterns of TXF-TCNQ (X = S, Se, Te) by carrying out ab initio SCF-MO/MP2 calculations on appropriate model systems. The electrical conductivity of TXF-TCNQ increases as X varies from S to Se to Te. This increase is primarily caused by the conductivity enhancement in the donor stacks. In TXF-TCNQ (X = S, Se) the C-H bonds of both the donor and the acceptor molecules make intermolecular contacts shorter than the van der Waals radii sums, but in TTeF-TCNQ only the C-H bonds of the donor molecules do. This difference in the packing patterns was rationalized on the basis of the C-H...X and N(sp)...X (X = S, Se, Te) contact interaction energies estimated by ab initio SCF-MO/MP2 calculations on H₃C-H...XH₂ and H-C≡N...XH₂.

INTRODUCTION

For nearly two decades synthetic organic chemistry has provided a vital means for probing the field of solid state chemistry. From the prototypical system, tetrathiafulvalene-tetracyanoquinodimethane (TTF-TCNQ),¹ has developed a new branch of synthetic conductors whose electronic ground state spans the realm from semiconducting to superconducting. These narrow band quasi one and two dimensional systems have contributed significantly to the understanding of many

physical phenomena such as charge and spin density waves, Peierls transitions and Mott-Hubbard insulators to name a few.²

Initially the major thrust was to chemically increase the dimensionality of these systems in order to circumvent the Peierls transition (a pathological low dimensional metal-insulator transition) preserving the metallic ground state to low temperature and afford the possibility of superconductivity.^{3, 4} This was accomplished with hexamethylenetetraselenafulvalene (HMTSF)-TCNQ, which maintains semimetallic conductivity to low temperature without showing superconductivity.⁵ However, alternate chemical modifications to the fulvalene backbone produced tetramethyltetraselenafulvalene (TMTSF) and bis(ethylenedithio)tetrathiafulvalene (BEDT-TTF) which resulted in the low-temperature superconductors (TMTSF)₂X (X⁻ = ClO₄⁻) and (BEDT-TTF)₂X (X⁻ = I₃⁻, AuI₂⁻, IBr₂⁻, Cu(NCS)₂⁻).⁶

Strongly correlated to obtaining the superconducting ground state has been the increase of dimensionality created by the intra- and interstack chalcogen contacts. These contacts produce a two dimensional conduction net similar to those exhibited in the high temperature superconducting ceramics. With the introduction of tellurium into the fulvalene moiety with tetratellurafulvalene (TTeF),⁷ these contacts should be increased due to the spatially larger tellurium atomic orbitals. In addition, with this larger chalcogen the bandwidth should be increased, the on-site Coulombic repulsion reduced and the band filling changed producing materials with higher conductivities which remain metallic to low temperatures.

In this work, we report the crystal structure, the electrical conductivity, and the magnetic susceptibility of TTeF-TCNQ.^{7, 8} To compare the electrical conductivities of TXF-TCNQ (X = S, Se, Te), we then examine the widths of the donor (TXF) bands and the acceptor (TCNQ) bands by performing tight-binding band calculations⁹ based upon the extended Hückel method¹⁰. Finally, we study why the crystal structure of TTeF-TCNQ differs considerably from those of TTF-TCNQ and TSF-TCNQ on the basis of ab initio SCF-MO/MP2 calculations on model systems.

SYNTHESIS AND CRYSTAL STRUCTURE OF TTeF-TCNQ

Shiny black needles of TTeF-TCNQ have been prepared by carefully layering a carbon disulfide/TTeF solution with an acetonitrile/TCNQ solution (1-3mM each) in a straight and H cell. Because the carbon disulfide/TTeF solution is easily air oxidized and water sensitive, the crystals were grown in a glove box with an inert atmosphere

of high purity helium. High purity solvents (>99.9%) were dried and then fractionally distilled under argon before use. TTeF was purified via flash silica gel/carbon disulfide column. TCNQ was gradiently sublimed. Crystal dimensions for the conductivity measurements averaged $1.2 \times 0.01 \times 0.01 \text{ mm}^3$. They are very brittle and have a tendency to be branched. These tendencies produced a crystal which is mechanically weak and crystallographically imperfect. This may be due in part to the rapid growth afforded by the diffusion cell growth technique, the purity of donor and possible solvent inclusion.

TTeF-TCNQ crystallizes in the triclinic space group $P\bar{1}$ with unit cell parameters $a = 3.947(3) \text{ \AA}$, $b = 7.397(4) \text{ \AA}$, $c = 16.622(10) \text{ \AA}$, $\alpha = 86.58(5)^\circ$, $\beta = 83.27(6)^\circ$, $\gamma = 80.69(6)^\circ$ and $V_c = 475.3(6) \text{ \AA}^3$ with $Z=1$. Single crystal x-ray diffraction data were determined with monochromatic Mo $K\alpha$ radiation on a SYNTEX P2₁ 4-circle diffractometer equipped with a CRYSTAL LOGIC automation system. A total of 2355 diffracted intensities were measured ($4.0^\circ \leq 2\theta \leq 45.0^\circ$). These were averaged [$R(F) = 0.045$, $R_w(F^2) = 0.028$] to give 1242 independent reflections. The structure was solved with MULTAN and refined with full matrix least squares including anisotropic thermal parameters for all non-hydrogen atoms. Hydrogen atoms were included in the refinement at calculated positions with fixed isotropic temperature factors, $B_{\text{iso}} = 5.0 \text{ \AA}^2$. The 1127 reflections with $F > 0.0$ gave final agreement factors of $R(F) = 0.086$, $R_w(F^2) = 0.052$ and "Goodness of Fit" = 1.05. Positional parameters for TTeF-TCNQ are given in Table 1 while interatomic distances and angles appear in Table 2. The atom numbering schemes for TTeF and TCNQ are shown in Figures 1a and 1b, respectively.

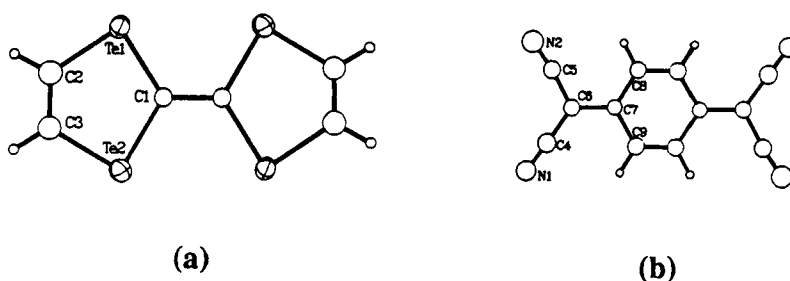


FIGURE 1 Atom numbering schemes for (a) TTeF and (b) TCNQ.

TABLE 1 Positional and equivalent isotropic thermal parameters for TTeF-TCNQ

Atom	x	y	z	$U_{eq} \cdot 10^4$ ^a
Te1	0.7197(3)	0.28830(14)	0.61447(6)	302(4)
Te2	0.5510(3)	0.76830(15)	0.58185(7)	334(5)
C1	0.543(4)	0.509(2)	0.5392(9)	235(51)
C2	0.751(5)	0.464(2)	0.7036(10)	351(65)
C3	0.689(4)	0.652(2)	0.6925(10)	302(60)
C4	0.892(5)	0.332(2)	0.1167(11)	382(68)
C5	0.901(5)	0.039(2)	0.1904(9)	317(62)
C6	0.823(4)	0.145(2)	0.1207(10)	315(61)
C7	0.651(4)	0.071(2)	0.0596(9)	299(59)
C8	0.586(4)	-0.113(2)	0.0671(10)	300(60)
C9	0.559(4)	0.182(2)	-0.0109(8)	278(57)
N1	0.944(4)	0.475(2)	0.1193(9)	447(60)
N2	0.984(4)	-0.040(2)	0.2489(10)	530(67)

^a The complete temperature factor is $\exp(-8\pi^2 U_{eq} \sin^2 \theta / \lambda^2)$, where

$U_{eq} = 1/3 \sum_{ij} U_{ij} a_i^* a_j^* a_i a_j$ in units of \AA^2 .

TABLE 2 Interatomic distances and angles in TTeF-TCNQ

Atoms	Dist. (\AA)	Atoms	Dist. (\AA)	Atoms	Dist. (\AA)
Te1-C2	2.05(2)	Te1-C1	2.08(2)	Te2-C3	2.08(2)
Te2-C1	2.091(14)	C1-C1	1.40(3)	C2-C3	1.38(2)
C4-N1	1.11(2)	C4-C6	1.45(2)	C5-N2	1.15(2)
C5-C6	1.40(2)	C6-C7	1.46(2)	C7-C8	1.43(2)
C7-C9	1.44(2)	C8-C9	1.32(2)		

Atoms	Angle ($^\circ$)	Atoms	Angle ($^\circ$)	Atoms	Angle ($^\circ$)
C2-Te1-C1	90.4(6)	C3-Te2-C1	90.8(6)	C1-C1-Te1	123.8(14)
C1-C1-Te2	120.3(15)	Te1-C1-Te2	115.6(7)	C3-C2-Te1	123.0(13)
C2-C3-Te2	119.6(13)	N1-C4-C6	175.2(19)	N2-C5-C6	174.7(18)
C5-C6-C4	116.7(14)	C5-C6-C7	120.0(14)	C4-C6-C7	123.0(15)
C8-C7-C9	118.9(14)	C8-C7-C6	120.6(14)	C9-C7-C6	120.4(14)
C9-C8-C7	120.9(15)	C8-C9-C7	120.2(14)		

Projection views of the donor and the acceptor stacks of TTeF-TCNQ along the a- and b-axis directions are shown in Figures 2a and 2b, respectively. TTeF-TCNQ has layers of donor molecules which have intermolecular chalcogen...chalcogen contacts not only along the intrastack but also along the interstack directions. These donor layers alternate with layers of acceptor molecules. This mode of packing, typically found for most (TMTSF)₂X and (BEDT-TTF)₂X salts, is quite different from that of TXF-TCNQ ($X = S, Se$). As depicted in Figures 3a and 3b, the TXF-TCNQ ($X = S, Se$) salts have donor stacks separated by acceptor stacks so that there exist no short chalcogen...chalcogen contacts between donor stacks. In addition, the adjacent acceptor and donor molecules are locked in an "X"-type arrangement (Figure 3b).

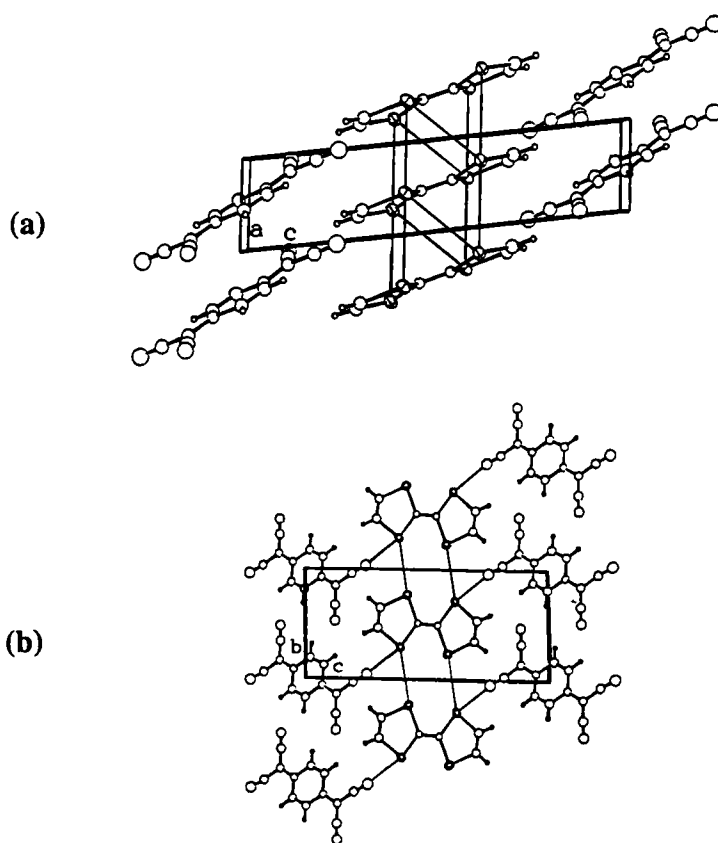


FIGURE 2 Projection views of the donor and acceptor stacks of TTeF-TCNQ along the a- and b-axis directions in (a) and (b), respectively.

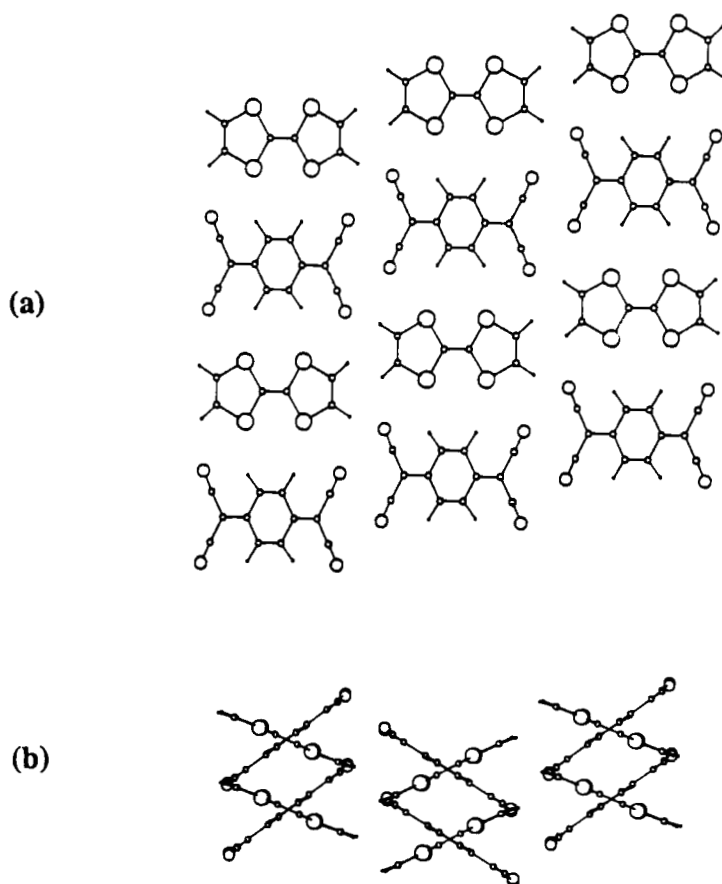


FIGURE 3 Projections views of the donor and acceptor stacks of TXF-TCNQ (X=S, Se) along the b- and a-axis directions in (a) and (b), respectively.

PHYSICAL PROPERTIES OF TTeF-TCNQ

The room temperature dc conductivity of crystalline TTeF-TCNQ needles averages $2200 \pm 300 (\Omega\text{-cm})^{-1}$ (25 samples). The main reason for the large scatter in the conductivities is attributed to the inaccuracies in measuring the cross sectional area of these small crystals and marked differences from batch to batch as the quality of the donor increased. (One batch of 3 samples exhibited room temperature values of $3300 (\Omega\text{-cm})^{-1}$.) Electrical contacts were made from the crystal to the sample board contacts by attaching 3-5 mm kinked 12.7 micron diameter gold wires in a floating four-probe configuration with Dupont 4929 silver paste with 2-butoxyethyl acetate

thinner. The current contacts completely enclosed the ends and the voltage contacts completely circled the crystal. Room temperature resistances were typically 2-20 Ω with contact resistances around 25 Ω . No spurious nested voltages, indicative of fractured crystals and/or bad contacts, were observed at room temperature.¹²

Conductivity as function of temperature was measured down to <2K. The sample board was placed inside a quasi-isothermal copper can sample holder in a constant flow cryostat. Cooling rates as low as 0.1 K/min were used to collect data every ~ 0.02 K. A constant current of 30 μA (deviations from Ohmic behavior were not observed until ~ 300 μA) was used.

Sudden drops in the conductivity began occurring around 160 K. When these sudden drops were removed from the data (assuming the conductivity is essentially the same before and after the drop and is solely a manifestation of the change of the geometric shape factor) it can be seen that the conductivity is increasing down to 2 K leading to a conductivity that is 9.5 times the room temperature value (See Figure 4). Below 2 K the jumps could not be removed using the above assumption. Rf penetration depth measurements on TTeF-TCNQ revealed no superconductivity at ambient pressure down to 0.55 K.

Magnetic susceptibility measurements used fine (< 0.2 mm in length) crystallites grown from slightly concentrated solutions. The magnetic susceptibility χ of TTeF-TCNQ is nearly temperature-independent. This Pauli-like paramagnetic behavior of the χ is consistent with the metallic properties of TTeF-TCNQ.

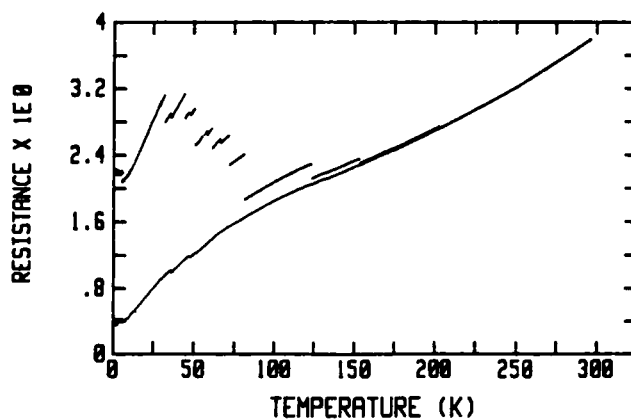


FIGURE 4 Electrical resistivity of TTeF-TCNQ as a function of temperature.

SIMILARITY AND DIFFERENCES IN TXF-TCNQ (X = S, Se, Te)**A. ELECTRONIC STRUCTURES**

Several important physical parameters of TXF-TCNQ (X = S, Se, Te) are summarized in Table 3. As X varies from S to Se to Te, the stacking axis length increases as does the amount of charge transfer $z(e^-)$ from TXF to TCNQ increases. These trends are understandable in terms of increased chalcogen size and changes in the ionization potentials of TXF in combination with the increased donor polarizability.

TABLE 3 Physical parameters of TXF-TCNQ (X=S, Se, Te)

Parameter	X=S	X=Se	X=Te	
$\sigma_{300K}(\Omega \text{ cm})^{-1}$	500±100 ^a	800±100 ^e	2200±300	
$\sigma_{\text{max}} / \sigma_{300K}$	~14 ^a	~12 ^e	~9.5 ^f , ~3g,h	
T _{max} (K)	59±1 ^a	40±1 ^e	~2 ^f , 100g	
Stacking axis (Å)	3.819 ^b	3.876 ^e	3.947	
z(e ⁻)	0.59 ^c	0.63 ^c	0.71±0.03 ^h	
$\chi_{300K}(\times 10^{-4} \text{ emu/mol})$	4.0 ^d	3.0 ^c	-1.9±0.1 ⁱ	
^a Refs. 1 and 19	^b Ref. 20	^c Ref. 21	^d Ref. 22	^e Ref. 23
^f dc-conductivity	^g microwave-conductivity	^h Ref. 7	ⁱ χ vs H data	

To compare the electronic properties of TXF-TCNQ (X = S, Se, Te), we performed tight-binding band electronic structure calculations on isolated donor and acceptor stacks of TXF-TCNQ and on an isolated donor layer of TTeF-TCNQ by employing both single- and double-zeta Slater type orbitals.¹³ These calculations show that all the TXF-TCNQ salts are quasi one-dimensional metals. For example, Figure 5a shows the dispersion relation of the highest occupied band calculated for a donor layer of TTeF-TCNQ by using the double-zeta orbitals. The dashed line of Figure 5a refers to the Fermi level appropriate for $z(e^-) = 0.71$. The Fermi surface associated with this band, shown in Figure 5b, is not closed so that each donor layer of TTeF-TCNQ is a one-dimensional metal. With the single-zeta orbitals, the

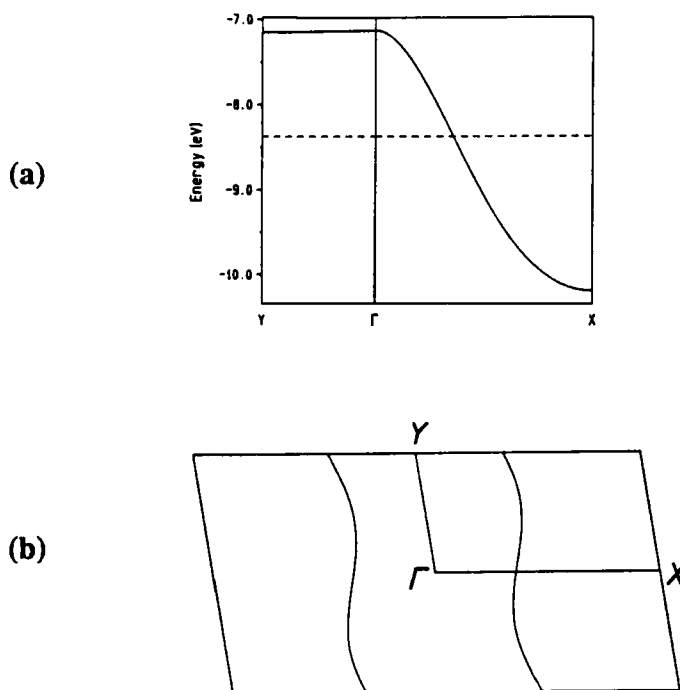


FIGURE 5 (a) Dispersion relation of the highest occupied band calculated for a TTeF layer, where the Fermi level is appropriate for the charge transfer $z(e^-)$ of 0.71. (b) Fermi surface associated with the partially filled band of Figure 5a.

interactions between donor stacks become weaker causing the Fermi surface to become flatter than that of Figure 5b.

Table 4 summarizes the calculated widths of the donor and the acceptor bands (i.e., W_D and W_A , respectively) for TXF-TCNQ ($X = \text{S, Se, Te}$) by using the single- and double-zeta orbitals. As is well known, the double-zeta bandwidths are about two times larger than the corresponding single-zeta values. Nevertheless, it is important to observe from both calculations that the acceptor band width W_A remains practically the same but the donor bandwidths W_D gradually increases as X changes from S to Se to Te. Let us now examine how the electrical conductivities of TXF-TCNQ can be related to the bandwidths W_D and W_A . Let $\sigma(X)$ represent the electrical conductivity of TXF-TCNQ ($X = \text{S, Se, Te}$) at 300 K. Table 3 shows that the $\sigma(\text{S})$: $\sigma(\text{Se})$: $\sigma(\text{Te})$ ratio is 1: 1.2-2.3 : 3.2 - 6.3. For a system with one partially filled band, the electrical conductivity σ is related to the band width W as $\sigma \propto W^2$.

TABLE 4 Calculated bandwidths W_D and W_A (eV) of TXF-TCNQ (X=S, Se, Te)^a

Salt	W_D	W_A
X=S	0.30 (0.85)	0.66 (1.37)
X=Se	0.44 (1.52)	0.62 (1.31)
X=Te	1.30 (2.49)	0.64 (1.36)

^a Numbers without parentheses refer to the bandwidths calculated with the single-zeta Slater type orbitals, and those in parentheses to those obtained with the double-zeta Slater type orbitals.

Each TXF-TCNQ salt consists of two partially filled bands, one resulting from the HOMO of TXF and the other from the LUMO of TCNQ. Therefore, the electrical conductivity $\sigma(X)$ is expected to be related to W_D and W_A as $\sigma(X) \propto W_D^2 + W_A^2$. Accordingly, the $\sigma(S) : \sigma(Se) : \sigma(Te)$ ratio is calculated to be 1 : 1.1 : 4.0 by the single-zeta bandwidths and 1 : 1.5 : 3.1 by the double-zeta bandwidths. These calculated ratios are in excellent agreement with the experimental ratio 1 : 1.2 - 2.3 : 3.2 - 6.3. Therefore the conductivity increase in the series TXF-TCNQ is due primarily to the conductivity enhancement in the donor stacks.

B. INTERMOLECULAR CONTACTS

The crystal packing patterns of the organic donor salts (BEDT-TTF)₂X and their analogs are largely governed by the short intermolecular contact interactions involving the C-H bonds (i.e., the C-H...donor and C-H...anion contacts).^{14, 15} Thus it is of importance to examine the short intermolecular contacts present in TXF-TCNQ (X = S, Se, Te). The intermolecular chalcogen...chalcogen contact (e.g., S...S, Se...Se) interactions are repulsive in nature,¹⁵ so we exclude such interactions from our consideration in the following.

Figure 6 shows a perspective view of the short intermolecular contacts between the donor and the acceptor molecules in TXF-TCNQ (X = S, Se). These contacts consist of the C-H (donor)⋯N(sp) contacts (2.52, 2.76 and 2.78 Å for X = S, and 2.68, 2.85 and 2.94 Å for X = Se), the C-H (acceptor)⋯X contacts (2.93 and 2.9 Å for X = S, and 2.90 and 2.98 Å for X = Se), and the N(sp)⋯X contacts (3.20 and 3.25 Å for X = S, and 3.17 and 3.18 Å for X = Se). Figure 7 shows a perspective view of the short intermolecular contacts between the donor and the acceptor molecules of TTeF-TCNQ. These contacts consist of the C-H (donor)⋯N(sp) contacts (2.57, 2.73 and 2.73 Å) and the N(sp)⋯Te contact (3.08 Å). Therefore, as in the case of the (BEDT-TTF)₂X salts and their analogs, the intermolecular contacts shorter than the van der Waals radii sums in TXF-TCNQ (X = S, Se, Te) are dominated by those involving the C-H bonds. In TXF-TCNQ (X = S, Se) both the donor and the acceptor C-H bonds participate in short intermolecular contact interactions, while in TTeF-TCNQ only the donor C-H bonds do.

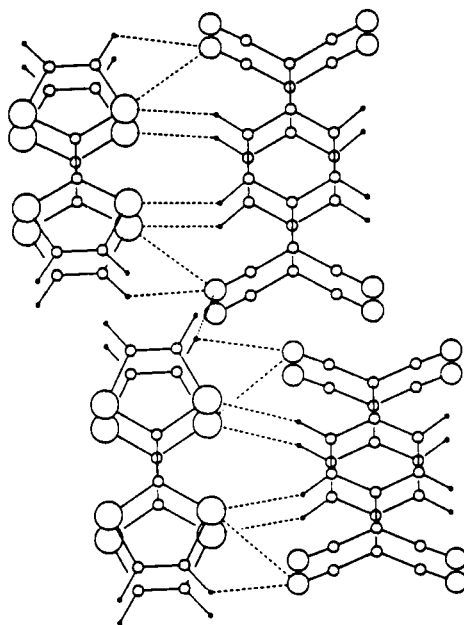


FIGURE 6 Perspective view of the short intermolecular C-H ⋯ X and N(sp) ⋯ X contacts in TXF-TCNQ (X=S, Se) (shown by dashed lines).

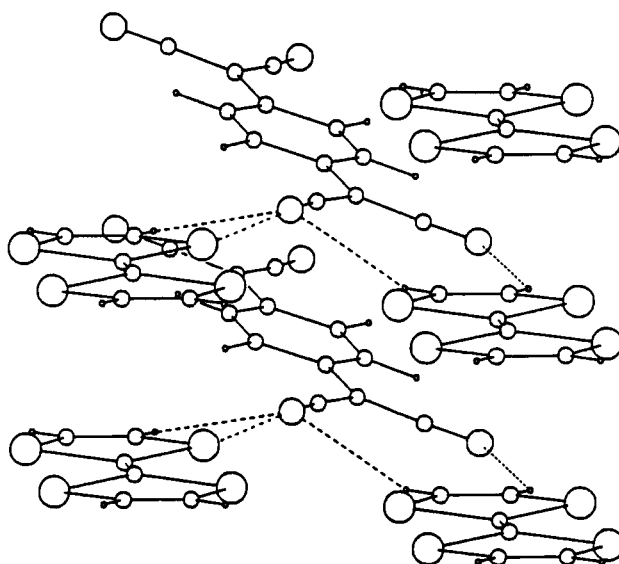


FIGURE 7 Perspective view of the short intermolecular C-H...Te and N(sp)...Te contacts in TTetF-TCNQ (shown by dashed lines).

Ab initio SCF-MO/MP2 calculations on $\text{H}_3\text{C-H}\cdots\text{XH}_2$ ($\text{X} = \text{S}, \text{Se}, \text{Te}$) suggested that the C-H...X contact interactions are attractive in nature,¹⁵ as listed in Table 5. Here r_{opt} is the calculated optimum H...X distance, and ΔE is the dissociation energy calculated at r_{opt} . To examine the nature of the C-H...N(sp) and the N(sp)...Te contact interactions, we carry out ab initio SCF-MO/MP2 calculations on $\text{H}_3\text{C-H}\cdots\text{N}\equiv\text{C-H}$ (with C_{3v} symmetry) and $\text{H-C}\equiv\text{N}\cdots\text{XH}_2$ ($\text{X} = \text{S}, \text{Se}, \text{Te}$) (with C_{2v} symmetry) as a function on the H...N and N...X distances, respectively (by employing the 3-21G basis sets for H, C, N, and S¹⁶ and the [2s, 2p] set contracted from (3s, 3p) for Se and Te¹⁷ with the XH_2 ($\text{X}=\text{S}, \text{Se}, \text{Te}$) geometries of Ref. 15 and the $\text{H-C}\equiv\text{N}$ geometry of $\text{H-C} = 1.063 \text{ \AA}$ and $\text{C-N} = 1.155 \text{ \AA}$ ¹⁸). The ΔE and r_{opt} values calculated for the C-H...N(sp) and N(sp)...Te contacts are also listed in Table 5. The ΔE and r_{opt} values for the N(sp)...X ($\text{X} = \text{S}, \text{Se}$) contacts are not listed in Table 5, since the $\text{H-C}\equiv\text{N}\cdots\text{XH}_2$ ($\text{X} = \text{S}, \text{Se}$) are not calculated to be bound.

The C-H...N(sp) interaction is more attractive than the N(sp)...Te interaction, which in turn is more attractive than the C-H...X ($\text{X} = \text{S}, \text{Se}, \text{Te}$) interaction. (The attractive nature of the N(sp)...Te interaction originates from the fact that the net atomic charge of Te in H_2Te is positive, while that of N(sp) in $\text{H-C}\equiv\text{N}$ is negative.

TABLE 5 Optimum distances r_{opt} (Å) and dissociation energy ΔE (kcal/mol) associated with several intermolecular contacts

Contacts	r_{opt}	ΔE
C-H ... S	3.05	0.52
C-H ... Se	3.45	0.28
C-H ... Te	3.75	0.27
C-H ... N(sp)	2.58	2.29
N(sp) ... Te	3.85	0.97

In contrast, the net atomic charge of X in H_2X (X = S, Se) is negative.) Thus the packing pattern of of TTeF-TCNQ is dominated by the attractive C-H (donor)⋯N(sp) and N(sp)⋯Te interactions. Absence of such a packing pattern in TXF-TCNQ (X = S, Se) may be due in part to the non-attractive nature of the N(sp)⋯X (X = S, Se) interaction. The "X"-type locking between the adjacent donor and acceptor molecules of TXF-TCNQ (X = S, Se) (see Figure 3b) allows both the donor and acceptor molecule C-H bonds to engage in attractive intermolecular contact interactions.

In TTeF-TCNQ, C-H (donor)⋯N(sp) and N(sp)⋯Te contacts shorter than the van der Waals radii sums do not occur along the stacking direction. This reflects the fact that the stacking axis length of TTeF-TCNQ is large to accommodate the Te⋯Te contacts along the stacks. Thus, the intermolecular contact interactions are weak along the stacking direction, which may cause the brittle nature of the TTeF-TCNQ crystals.

CONCLUDING REMARKS

In the present work we compared the structural and electronic properties of the TXF-TCNQ (X = S, Se, Te) salts. Our tight-binding band calculations on TXF-TCNQ show that the acceptor bandwidth W_A remains nearly constant but the donor band width W_D increases as X varies from S to Se to Te. The experimental conductivity ratio $\sigma(\text{S})$: $\sigma(\text{Se})$: $\sigma(\text{Te})$ is very well reproduced by the relationship $\sigma(\text{X}) \propto W_D^2 + W_A^2$. Thus the increase in $\sigma(\text{X})$, which occurs when X changes from S to Se to Te,

is primarily caused by the conductivity enhancement in the TXF donor stacks. The crystal packing pattern of TTeF-TCNQ differs substantially from that of TXF-TCNQ ($X = S, Se$): In TXF-TCNQ ($X = S, Se$) the C-H bonds of both the donor and the acceptor molecules engage in short intermolecular contact interactions, while in TTeF-TCNQ only the C-H bonds of the donor molecules do. The differences in the packing patterns of TXF-TCNQ ($X = S, Se, Te$) can be rationalized in terms of the $C-H \cdots X$ ($X = S, Se, Te$) and the $N(sp) \cdots X$ ($X = S, Se, Te$) interaction energies obtained by ab initio SCF-MO/MP2 calculations.

ACKNOWLEDGMENT

Work at North Carolina State University and Argonne National Laboratory is supported by the U. S. Department of Energy, Office of Basic Energy Sciences, Division of Materials Sciences, under Grant DE-FG05-86ER45259 and Contract W-31-109-ENG-38, respectively. Work at the Johns Hopkins University was supported by the National Science Foundation-Solid State Chemistry Program grant DMR-8615305. We thank Dr. P. M. Grant for providing us with the crystal coordinates of TSF-TCNQ. J. J. N. thanks NATO and Ministerio de Educacion y Ciencia (Spain) for Fellowships which made it possible to visit North Carolina State University.

REFERENCES

1. J. P. Ferraris, D. O. Cowan, V. Walatka, Jr. and J. H. Perlstein, J. Am. Chem. Soc. **95**, 948 (1973).
2. D. O. Cowan and F. M. Wiygul, Chem. Eng. News, **64**, 28 (1986).
3. D. Cowan, P. Shu, C. Hu, W. Krug, T. Curruthers, T. Poehler and A. N. Bloch, The Chemistry and Physics of One-Dimensional Metals, H. J. Keller, ed., Plenum Press, NY, 1977, p. 25.
4. A. N. Bloch, T. F. Carruthers, T. O. Poehler and D. O. Cowan, The Chemistry and Physics of One-Dimensional Metals, H. J. Keller, ed., Plenum Press, NY, 1977, p. 47.
5. A. N. Bloch, D. O. Cowan, K. Bechgaard, R. E. Pyle, R. H. Banks and T. O. Poehler, Phys. Rev. Lett. **34**, 1561 (1975).

6. For a review, see: J. M. Williams, H. H. Wang, T. J. Emge, U. Geiser, M. A. Beno, P. C. W. Leung, K. D. Carlson, R. J. Thorn, A. J. Schultz and M. -H. Whangbo, Prog. Inorg. Chem., **35**, 51 (1987).
7. M. D. Mays, R. D. McCullough, D. O. Cowan, T. O. Poehler, W. A. Bryden and T. J. Kistenmacher, Solid State Commun., **65**, 1089 (1988).
8. M. D. Mays, R. D. McCullough, A. B. Bailey, D. O. Cowan, W. A. Bryden, T. O. Poehler and T. J. Kistenmacher, Synt. Met., **27**, B493 (1988).
9. (a) M. -H. Whangbo, J. M. Williams, P. C. W. Leung, M. A. Beno, T. J. Emge, H. H. Wang, K. D. Carlson, and G. W. Crabtree, J. Am. Chem. Soc., **107**, 5815 (1985).
(b) M. -H. Whangbo and R. Hoffmann, J. Am. Chem. Soc., **100**, 6093 (1978).
10. (a) R. Hoffmann, J. Chem. Phys., **39**, 1397 (1963).
(b) A modified Wolfsberg-Helmholz approximation was employed to calculate the off-diagonal matrix elements of the effective Hamiltonian: J. H. Ammeter, H. -B. Bürgi, J. C. Thibeault, and R. Hoffmann, J. Am. Chem. Soc., **100**, 3686 (1978).
11. (a) T. J. Kistenmacher, T. E. Phillips and D. O. Cowan, Acta Crystallogr. **330**, 763 (1974).
(b) The crystal structure of TSF-TCNQ is isostructural with that of TTF-TCNQ^{11a} (P. M. Grant, private communication).
12. D. E. Schafer, F. Wudl, G. A. Thomas, J. P. Ferraris and D. O. Cowan, Solid State Commun., **14**, 347 (1974).
13. The double-zeta Slater type orbitals were taken from: E. Clementi and C. Roetti, At. Data Nucl. Data Tables, **14**, 177 (1974).
14. M. -H. Whangbo, D. Jung, J. Ren, M. Evain, J. J. Novoa, F. Mota, S. Alvarez, J. M. Williams, M. A. Beno, A. M. Kini, H. H. Wang, and J. R. Ferraro, The Physics and Chemistry of Organic Superconductors, G. Saito and S. Kagoshima, eds., Springer Verlag, in press.
15. J. J. Novoa, M. -H. Whangbo and J. M. Williams, This volume.
16. GAUSSIAN 86, M. J. Frish, J. S. Brinkley, H. B. Schlegel, K. Raghavachari, C. F. Melius, R. L. Martin, J. J. P. Stewart, F. W. Bobrowicz, C. M. Rohlfing, L. R. Kahn, D. J. Defrees, R. Seeger, R. A. Whiteside, D. J. Fox, E. M. Fleuder and J. A. Pople, Carnegie-Mellon Quantum Chemistry Publishing Unit, Pittsburgh, PA 1984.
17. W. R. Wadt and P. J. Hay, J. Chem. Phys., **82**, 284 (1985).

18. J. K. Tyler and J. Sheridan, Trans. Far. Soc., **59**, 2661 (1963).
19. G. A. Thomas et al., Phys. Rev. B, **13**, 5105 (1976).
20. T. J. Kistenmacher, T. E. Phillips, and D. O. Cowan, Acta Crystallogr. Sect. B, **30**, 763 (1973).
21. J. S. Chappel, A. N. Bloch, W. A. Bryden, M. Maxfield, T. O. Poehler and D. O. Cowan, J. Am. Chem. Soc., **103**, 2442 (1981).
22. J. C. Scott, A. F. Garito and A. J. Heeger, Phys. Rev. B, **10**, 3131 (1974).
23. S. Etemad, T. Penney, E. M. Engler, B. A. Scott, and P. E. Seiden, Phys. Rev. Lett. **30**, 741 (1975).